Synthesis, Structural Characterization, and Ethylene Polymerization Behavior of the Vanadium(III) Complexes Bearing Salicylaldiminato Ligands

Ji-Qian Wu,[†,‡] Li Pan,[†] Ning-Hai Hu, and Yue-Sheng Li*[,†]

State Key Laboratory of Polymer Physics and Chemistry, Changchun Institute of Applied Chemistry, Chinese Academy of Sciences, Changchun 130022, People's Republic of China, and Changchun Branch of Graduate School of the Chinese Academy of Sciences, People's Republic of China

Received February 3, 2008

Vanadium(III) complexes bearing salicylaldiminato ligands (**2a**−**k**) [RN═CH(ArO)]$VCl_2(THF)_2$ (Ar = C_6H_4, R = Ph, **2a**; *p*-CF_3Ph, **2b**; *p*-CH_3Ph, **2c**; 2,6-Me_2Ph, **2d**; 2,6-*i*Pr_2Ph, **2e**; cyclohexyl, **2f**; Ar = C_6H_3tBu(2), R = Ph, **2g**; 2,6-*i*Pr_2Ph, **2h**; Ar = $C_6H_2t$$Bu_2$(2,4), R = Ph, **2i**; 2,6-*i*Pr_2Ph, **2j**; Ar = $C_6H_2Br_2$, R = Ph, **2k**) were prepared from $VCl_3(THF)_3$ by treating with 1.0 equiv of (RN═CH)ArOH in tetrahydrofuran (THF) in the presence of excess triethylamine (TEA). The reaction of $VCl_3(THF)_3$ with 2.0 equiv of (RN═CH)ArOH in THF in the presence of excess TEA afforded vanadium(III) complexes bearing two salicylaldiminato ligands (**3a**−**k**), [RN═CH(ArO)]$_2$VCl$(THF)_x$ (Ar = C_6H_4, x = 1, R = Ph, **3a**; *p*-CF_3Ph, **3b**; *p*-CH_3Ph, **3c**; 2,6-Me_2Ph, **3d**; 2,6-*i*Pr_2Ph, **3e**; cyclohexyl, **3f**; Ar = C_6H_3tBu(2), x = 1, R = Ph, **3g**; x = 0, 2,6-*i*Pr_2Ph, **3h**; Ar = $C_6H_2t$$Bu_2$(2,4), x = 1, R = Ph, **3i**; 2,6-*i*Pr_2Ph, x = 0, **3j**; Ar = $C_6H_2Br_2$, x = 1, R = Ph, **3k**). These complexes were characterized by FTIR and mass spectra as well as elemental analysis. Structures of complexes **2a**, **2b**, **2g**, **2i**, **2k**, **3b**, **3c**, **3e**, **3j**, and **3k** were further confirmed by X-ray crystallographic analysis. The complexes were investigated as catalysts for ethylene polymerization in the presence of Et_2AlCl. Complexes **2a**−**k** exhibited high catalytic activities (up to 22.3 kg PE/mmol$_V$·h·bar) and afforded high molecular weight polymers (M_w > 100 kg/mol) with unimodal molecular weight distributions at room temperature, while displaying relatively low catalytic activities, and produced polymers with low molecular weight (M_w < 30 kg/mol) and broad molecular weight distributions at 70 °C. Complexes **3a**−**k** were also effective catalyst precursors for ethylene polymerization. Even at 70 °C these complexes produced polyethylenes with unimodal distributions. These results indicated that the structural model of the salicylaldiminato vanadium(III) complexes greatly affected the ethylene polymerization behaviors.

Introduction

A significant number of advances in olefin polymerization catalysis have been reported in the past decade, and the development of new generation "non-metallocene" catalysts has attracted great interest recently.[1] Among the transition metals, vanadium catalysts exhibited promising characteristics,[2–19] especially for the syntheses of high molecular weight polyethylene,[2,3] syndiotactic polypropylene,[5] and poly(ethylene-*co*-propylene) and poly(ethylene-*co*-propylene-*co*-diene) elastomers.[4] Therefore, the design and synthesis of new vanadium complexes as olefin polymerization catalysts has attracted considerable attention. Recently, modification of the ligand frameworks of

* To whom correspondence should be addressed. Fax: +86-431-5262124. E-mail: ysli@ciac.jl.cn.

† State Key Laboratory of Polymer Physics and Chemistry.

‡ Changchun Branch of Graduate School of the Chinese Academy of Sciences.

(1) (a) Domski, G. J.; Rose, J. M.; Coates, G. W.; Bolig, A. D.; Brookhart, M. *Prog. Polym. Sci.* **2007**, *32*, 30. (b) Gibson, V. C.; Spitzmesser, S. K. *Chem. Rev.* **2003**, *103*, 283.

(2) Natta, G.; Pasquon, I.; Zambelli, A. *J. Am. Chem. Soc.* **1962**, *84*, 1488.

(3) (a) Carrick, W. L. *J. Am. Chem. Soc.* **1958**, *80*, 6455. (b) Carrick, W. L.; Kluiber, R. W.; Bonner, E. F.; Wartman, L. H.; Rugg, F. M.; Smith, J. J. *J. Am. Chem. Soc.* **1960**, *82*, 3883. (c) Lehr, M. H.; Carmen, C. J. *Macromolecules* **1969**, *2*, 217. (d) Lehr, M. H. *Macromolecules* **1968**, *1*, 178.

(4) (a) Christman, D. L.; Keim, G. I. *Macromolecules* **1968**, *1*, 358. (b) Doi, Y. ; Tokuhiro, N. ; Nunomura, M. ; Miyake, H. ; Suzuki, S. ; Soga, K. In *Transition Metals and Organometallics as Catalysts for Olefin Polymerization*; Kaminsky, W., Sinn, H., Eds.; Springer-Verlag: Berlin, 1988; p379. (c) Doi, Y.; Suzuki, S.; Soga, K. *Macromolecules* **1986**, *19*, 2896. (d) Addisson, E. J. *Polym. Sci., Part A: Polym. Chem.* **1994**, *32*, 1033. (e) Davis, S. C.; von Hellens, W.; Zahalka, H. In *Polymer Material Encylopedia*; Salamone, J. C., Ed.; CRC Press Inc., 1996; Vol. 3.

(5) (a) Zambelli, A.; Pasquon, I.; Signorini, R.; Natta, G. *Makromol. Chem.* **1968**, *112*, 160. (b) Zambelli, A.; Natta, G.; Pasquon, I.; Signorini, R. J. *Polym. Sci., Part C* **1967**, *16*, 2485. (c) Doi, Y.; Kinoshita, J.; Morinaga, A.; Keii, T. J. *Polym. Sci., Polym. Chem. Ed.* **1975**, *13*, 2491.

(6) Related reviews:(a) Hagen, H.; Boersma, J.; van Koten, G. *Chem. Soc. Rev* **2002**, *31*, 357. (b) Gambarotta, S. *Coord. Chem. Rev.* **2003**, *237*, 229. (c) Bolton, P. D.; Mountford, P. *Adv. Synth. Catal.* **2005**, *347*, 355.

(7) (a) Chan, M.; Cole, J. M.; Gibson, V. C.; Howard, J. *Chem. Commun.* **1997**, 2345. (b) Chan, M.; Chew, K. C.; Dalby, C. I.; Gibson, V. C.; Kohlmann, A.; Little, I. R.; Reed, W. *Chem. Commun.* **1998**, 1673. (c) Tomov, A. K.; Gibson, V. C.; Zaher, D.; Elsegood, M.; Dale, S. H. *Chem. Commun.* **2004**, 1956.

(8) Kim, W. K.; Fevola, M. J.; Liable-Sands, L. M.; Rheingold, A. L.; Theopold, K. H. *Organometallics* **1998**, *17*, 4541.

(9) (a) Brussee, E.; Meetsma, A.; Hessen, B.; Teuben, J. H. *Organometallics* **1998**, *17*, 4090. (b) Brussee, E.; Meetsma, A.; Hessen, B.; Teuben, J. H. *Chem. Commun* **2000**, 497.

(10) (a) Ma, Y. L.; Reardon, D.; Gambarotta, S.; Yap, G. *Organometallics* **1999**, *18*, 2773. (b) Reardon, D.; Conan, F.; Gambarotta, S.; Yap, G.; Wang, Q. Y. *J. Am. Chem. Soc.* **1999**, *121*, 9318. (c) Jabri, A.; Korobkov, I.; Gambarotta, S.; Duchateau, R. *Angew. Chem., Int. Ed.* **2007**, *46*, 6119.

(11) (a) Hagen, H.; Bezemer, C.; Boersma, J.; Kooijman, H.; Lutz, M.; Spek, A. L.; van Koten, G. *Inorg. Chem.* **2000**, *39*, 3970. (b) Hagen, H.; Boersma, J.; Lutz, M.; Spek, A. L.; van Koten, G. *Eur. J. Inorg. Chem.* **2001**, *117*, 123.

10.1021/om800097b CCC: $40.75
Publication on Web 07/09/2008

vanadium complexes has led to impressive advances in catalyst productivity, thermal stability, and comonomer incorporation capability.[6–20] For example, Gambarotta and co-workers found that bis(imino)pyridine vanadium(III) complexes showed high catalytic activity toward ethylene polymerization and produced bimodal molecular weight distribution PEs.[10b] The bis(benzimidazole)amine vanadium catalysts reported by Gibson's group displayed high efficiency for ethylene (co)polymerization, affording high molecular weight polymers with unimodal distribution.[7c] Nomura demonstrated that high catalytic activity and efficient α-olefin or cycloolefin incorporation could be obtained if the (arylimino)(aryloxo)vanadium complexes were used as catalyst precursors.[17] Redshaw's group investigated various aryloxide-based vanadyl complexes, which exhibited excellent performance in olefin polymerization.[19] Recently, our group reported the synthesis and structural characterization of a type of vanadium catalyst featuring unsymmetrical bidentate *β*-enaminoketonato ligands, which revealed remarkable catalytic activity not only for ethylene polymerization but also for ethylene/α-olefin and ethylene/cycloolefin copolymerizations.[21]

Salicylaldiminato ligands have been used in transition metal organometallics and have already been shown to afford highly active olefin polymerization catalysts for group 4,[22] group 6,[23] and group 10[24] metal systems. For instance, it has been known that titanium/zirconium complexes containing bis(salicylaldiminato) ligands can be used to produce polyethylene or syndiotactic polypropylene with high molecular weight and narrow molecular weight distribution, and the catalytic behaviors were highly affected by the substituents on both the phenoxy and the imino groups.[25] However, the reports on the salicylaldiminato vanadium catalysts for olefin polymerization are limited so far.[19d,20a,b,26] In this paper, we investigated the synthesis and structural analysis of a series of salicylaldiminato vanadium complexes [RN=CH(ArO)]$VCl_2(THF)_2$ (**2a**−**k**) and bis(salicylaldiminato) vanadium complexes [RN=CH(ArO)]$_2$-$VCl(THF)_x$ (**3a**−**k**). We also present our preliminary results concerning their use as catalysts for ethylene polymerization in the presence of Et_2AlCl.

Scheme 1. General Synthetic Route of the Vanadium Complexes Used in This Study

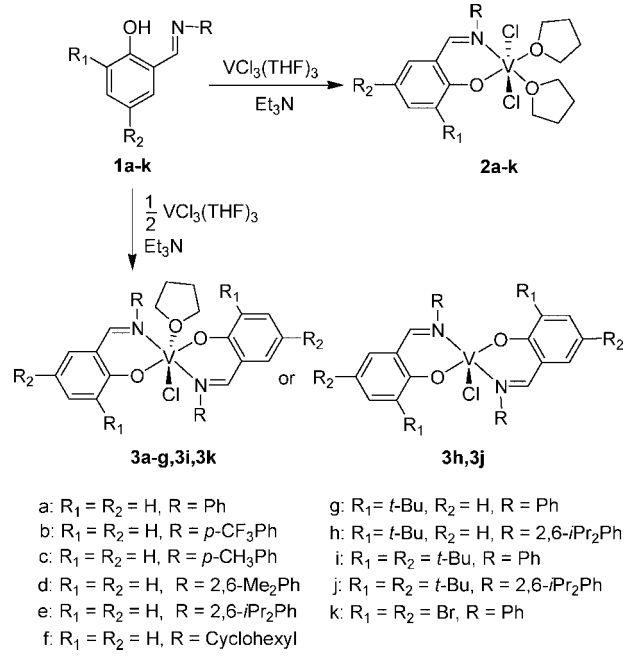

Results and Discussion

1. Synthesis and Characterization of Vanadium(III) Complexes [RN=CH(ArO)]$VCl_2(THF)_2$. A general synthetic route for new vanadium complexes used in this study is shown in Scheme 1. The reaction of $VCl_3(THF)_3$ with 1.0 equiv of (RN=CH)ArOH (**1a**−**k**) in tetrahydrofuran (THF) in the presence of excess TEA afforded vanadium(III) complexes **2a**−**k** in moderate to high yields (**2a**, 70%; **2b**, 70%; **2c**, 60%; **2d**, 63%; **2e**, 76%; **2f**, 69%; **2g**, 71%; **2h**, 53%; **2i**, 76%; **2j**, 64%; **2k**, 62%). These reactions took place along with evolution of hydrochloride, and the pure samples as dark red or brown crystallized solids were isolated from the chilled concentrated mixture of THF and hexane solution. These complexes were identified by FTIR and mass spectra as well as elemental analysis. In the EI/MS spectra of complexes **2**, there were no peaks of complexes **3** or 3:1 or 0:1 ligand-to-V(III) complexes, indicating the complexes display high purity. The resonances are broadened to such an extent that they become effectively unobservable in the ^1H (or ^{13}C) NMR spectra for these complexes in CD_2Cl_2 or C_6D_6, indicating that they are paramagnetic species.

(12) Takaoki, K.; Miyatake, T. *Macromol. Symp.* **2000**, *157*, 251.
(13) Zambelli, A.; Sessa, I.; Grisi, F.; Fusco, R.; Accomazzi, P. *Macromol. Rapid Commun.* **2001**, *22*, 297.
(14) (a) Colamarco, E.; Milione, S.; Cuomo, C.; Grassi, A. *Macromol. Rapid Commun.* **2004**, *25*, 450. (b) Cuomo, C.; Milione, S.; Grassi, A. J. *Polym. Sci., Part A: Polym. Chem.* **2006**, *44*, 3279.
(15) Liguori, D.; Centore, R.; Csok, Z.; Tuzi, A. *Macromol. Chem. Phys.* **2004**, *205*, 1058.
(16) Schmidt, R.; Welch, M. B.; Knudsen, R. D.; Gottfried, S.; Alt, H. G. J. *Mol. Catal. A: Chem.* **2004**, *222*, 17.
(17) (a) Nomura, K.; Sagara, A.; Imanishi, Y. *Macromolecules* **2002**, *35*, 1583. (b) Yamada, J.; Yamada, J.; Nomura, K. *Organometallics* **2005**, *24*, 2248. (c) Fujiki, M.; Nomura, K. *Organometallics* **2005**, *24*, 3621. (d) Wang, W.; Nomura, K. *Macromolecules* **2005**, *38*, 5905. (e) Wang, W.; Nomura, K. *Adv. Synth. Catal.* **2006**, *348*, 743. (f) Nomura, K.; Atsumi, T.; Fujiki, M.; Yamada, J. J. *Mol. Catal. A: Chem.* **2007**, *275*, 1.
(18) Bigmore, H. R.; Zuideveld, M. A.; Kowalczyk, R. M.; Cowley, A. R.; Kranenburg, M.; McInnes, E.; Mountford, P. *Inorg. Chem.* **2006**, *45*, 6411.
(19) (a) Redshaw, C.; Warford, L.; Dale, S. H.; Elsegood, M. *Chem. Commun.* **2004**, 1954. (b) Redshaw, C.; Rowan, M. A.; Homden, D. M.; Dale, S. H.; Elsegood, M.; Matsui, S.; Matsuura, S. *Chem. Commun.* **2006**, 3329. (c) Redshaw, C.; Rowan, M. A.; Warford, L.; Homden, D. M.; Arbaoui, A.; Elsegood, M.; Dale, S. H.; Yamato, T.; Casas, C. P.; Matsui, S.; Matsuura, S. *Chem.−Eur. J.* **2007**, *13*, 1090. (d) Homden, D. M.; Redshaw, C.; Hughes, D. L. *Inorg. Chem.* **2007**, *46*, 10827.
(20) (a) Nakayama, Y.; Bando, H.; Sonobe, Y.; Suzuki, Y.; Fujita, T. *Chem. Lett.* **2003**, *32*, 766. (b) Nakayama, Y.; Bando, H.; Sonobe, Y.; Fujita, T. J. *Mol. Catal. A: Chem.* **2004**, *213*, 141. (c) Casagrande, A.; Tavares, T.; Kuhn, M.; Casagrande, O. L.; dos Santos, J.; Teranishi, T. J. *Mol. Catal. A: Chem.* **2004**, *212*, 267. (d) Casagrande, A.; dos Anjos, P. S.; Gamba, D.; Casagrande, O. L.; dos Santos, J. J. *Mol. Catal. A: Chem.* **2006**, *255*, 19.
(21) Tang, L. M.; Wu, J. Q.; Duan, Y. Q.; Pan, L.; Li, Y. G.; Li, Y. S. *J. Polym. Sci., Part A: Polym. Chem.* **2008**, *46*, 2038.
(22) Suzuki, Y.; Terao, H.; Fujita, T. *Bull. Chem. Soc. Jpn.* **2003**, *76*, 1493.
(23) Jones, D. J.; Gibson, V. C.; Green, S. M.; Maddox, P. J.; White, A.; Williams, D. J. *J. Am. Chem. Soc.* **2005**, *127*, 11037.
(24) (a) Wang, C. M.; Friedrich, S.; Younkin, T. R.; Li, R. T.; Grubbs, R. H.; Bansleben, D. A.; Day, M. W. *Organometallics* **1998**, *17*, 3149. (b) Younkin, T. R.; Conner, E. F.; Henderson, J. I.; Friedrich, S. K.; Grubbs, R. H.; Bansleben, D. A. *Science* **2000**, *287*, 460. (c) Li, X. F.; Li, Y. S. *J. Polym. Sci. Part A: Polym. Chem.* **2002**, *40*, 2680.
(25) (a) Matsui, S.; Mitani, M.; Saito, J.; Tohi, Y.; Makio, H.; Matsukawa, N.; Takagi, Y.; Tsuru, K.; Nitabaru, M.; Nakano, T.; Tanaka, H.; Kashiwa, N.; Fujita, T. *J. Am. Chem. Soc.* **2001**, *123*, 6847. (b) Mitani, M.; Mohri, J.; Yoshida, Y.; Saito, J.; Ishii, S.; Tsuru, K.; Matsui, S.; Furuyama, R.; Nakano, T.; Tanaka, H.; Kojoh, S.; Matsugi, T.; Kashiwa, N.; Fujita, T. *J. Am. Chem. Soc.* **2002**, *124*, 3327. (c) Tian, J.; Coates, G. W. *Angew. Chem., Int. Ed.* **2000**, *39*, 3626. (d) Hustad, P. D.; Tian, J.; Coates, G. W. *J. Am. Chem. Soc.* **2002**, *124*, 3614.
(26) Milani, F.; Casellato, U.; Vigato, P. A.; Vidali, M.; Fenton, D. E.; Leal Gonzalez, M. S. *Inorg. Chim. Acta* **1985**, *103*, 15.

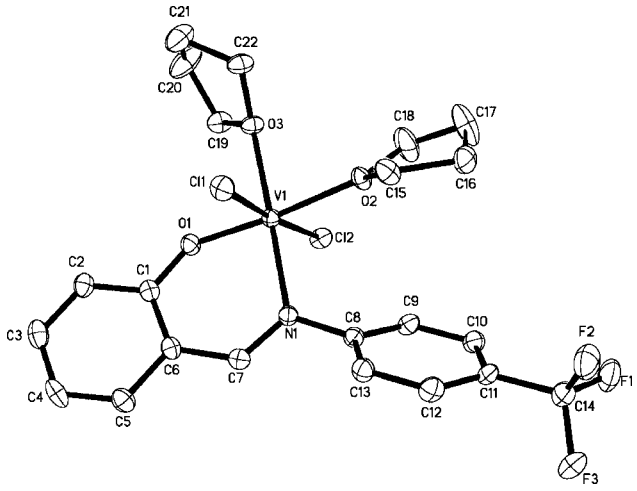

Figure 1. ORTEP drawing for complex **2b**. Thermal ellipsoids are drawn at the 30% probability level, and H atoms are omitted for clarity.

Crystals suitable for crystallographic analysis were grown from the THF−hexane mixture solution containing compounds **2a**, **2b**, **2g**, **2i**, and **2k**, respectively, and their molecular structures were further confirmed by X-ray crystallographic analysis as the monomeric species. The molecular structure of **2b** is shown in Figure 1, and those of **2a**, **2g**, **2i**, and **2k** are shown in Figure S1-4 in the Supporting Information, respectively. As shown in Figure 1, complex **2b** has a six-coordinate distorted octahedral geometry around the V metal center. The two chlorine atoms are situated in the *trans* position, while the two THF molecules are in *cis* position to each other, as seen in the bond angles for Cl(1)−V−Cl(2) (174.7°) and O(2)−V−O(3) (86.78°). These bond angles are somewhat analogous to those for vanadium complex $[PhN{=}C(CH_3)CHC(CF_3)O]VCl_2(THF)_2$ [Cl(1)−V−Cl(2) (175.49°) and O(2)−V−O(3) (86.96°)], reported previously.[21] The V−Cl bond distances (2.3639, 2.3509 Å) are also close to values reported previously.[8,9,21,27]

The molecular structures of complexes **2a** and **2g** are similar to that of complex **2b**, but there are some differences among complexes **2a**, **2i**, and **2k** (Table 1). For example, the O(1)−V−O(2) (171.75°), O(2)−V−O(3) (83.22°), and Cl(1)−V−Cl(2) (170.47°) bond angles in complex **2i** are smaller than those in **2a** (176.79°, 89.71°, and 174.75°), and the V−N(1) (2.069 Å) and V−O(1) (1.853 Å) bond distances in **2i** are somewhat shorter than those in **2a** (2.110 and 1.868 Å). In complex **2k**, the Cl(1)−V−Cl(2) (177.18°) bond angle is larger than that in complex **2a** (174.75°), while the V−O(1) (1.881 Å) bond distance is slightly longer than that in complex **2a** (1.868 Å). These differences result from the steric and electronic effects of the substituents in the aryloxy group (two *t*Bu in **2i** and two Br in **2k**).

2. Synthesis and Characterization of Vanadium(III) Complexes $[RN{=}CH(ArO)]_2VCl(THF)_x$. As shown in Scheme 1, reaction of $VCl_3(THF)_3$ with 2 equiv of salicyladimine ligands **1a**−**k** in the presence of excess TEA in THF afforded bis(salicyladiminato) complexes **3a**−**k** in moderate yields (**3a**, 64%; **3b**, 51%; **3c**, 69%; **3d**, 30%; **3e**, 66%; **3f**, 62%; **3g**, 42%; **3h**, 56%; **3i**, 65%; **3j**, 61%; **3k**, 80%). The reaction products were identified by mass spectra, FTIR, and elemental analysis. Similar to the case of complexes **2**, in the EI/MS spectra of complexes **3**there were also no peaks of complexes **2** or 3:1 or 0:1 ligand-to-V(III) complexes. ^{1}H NMR spectra indicated that these complexes are also paramagnetic species, which is similar to the case of complexes **2a**−**k**.

Table 1. Selected Bond Distances (Å) and Angles (deg) for Complexes 2a, 2b,2g, 2i, and 2k

	2a	2b	2g	2i	2k
			Bond Distances		
V−N(1)	2.1099(18)	2.116(3)	2.104(6)	2.069(3)	2.107(2)
V−O(1)	1.8684(16)	1.865(2)	1.858(5)	1.853(3)	1.8813(19)
V−O(2)	2.1379(16)	2.105(2)	2.105(5)	2.164(3)	2.0931(19)
V−O(3)	2.1140(16)	2.135(2)	2.137(5)	2.119(3)	2.1203(19)
V−Cl(1)	2.3639(7)	2.3638(10)	2.366(2)	2.3527(14)	2.3581(8)
V−Cl(2)	2.3509(7)	2.3738(10)	2.352(2)	2.3421(14)	2.3525(8)
			Bond Angles		
O(1)−V−O(2)	176.79(6)	175.02(10)	175.5(2)	171.75(12)	174.99(8)
O(1)−V−O(3)	87.08(7)	89.30(10)	89.9(2)	88.54(12)	90.02(8)
O(1)−V−N(1)	89.58(7)	89.11(10)	89.7(2)	88.91(13)	89.18(8)
O(1)−V−Cl(1)	92.70(6)	91.11(8)	93.15(16)	94.86(10)	90.82(7)
O(1)−V−Cl(2)	87.73(5)	93.94(8)	91.59(16)	94.56(10)	92.00(7)
O(2)−V−O(3)	89.71(7)	86.78(9)	85.97(19)	83.22(11)	85.00(8)
O(2)−V−Cl(1)	87.21(5)	85.98(7)	88.49(15)	85.66(8)	89.56(6)
O(2)−V−Cl(2)	87.73(5)	88.88(7)	86.62(15)	85.23(8)	87.62(6)
O(3)−V−Cl(1)	90.23(5)	92.21(7)	87.31(15)	91.99(9)	88.88(6)
O(3)−V−Cl(2)	88.33(5)	86.32(7)	90.50(15)	89.70(9)	90.96(6)
N(1)−V−O(2)	93.63(7)	94.85(10)	94.4(2)	99.34(12)	95.78(8)
N(1)−V−O(3)	174.62(7)	178.19(10)	179.5(2)	177.41(13)	177.64(8)
N(1)−V−Cl(1)	94.13(5)	88.69(8)	92.98(17)	87.81(10)	93.35(6)
N(1)−V−Cl(2)	87.59(5)	92.92(8)	89.25(17)	90.92(10)	86.84(6)
Cl(1)−V−Cl(2)	174.75(3)	174.72(4)	174.77(10)	170.47(5)	177.18(3)

Table 2. Selected Bond Distances (Å) and Angles (deg) for Complexes 3b, 3c, 3e, 3j, and 3k

	3b	3c	3e	3j	3k
			Bond Distances		
V−N(1)	2.122(3)	2.1290(18)	2.187(2)	2.117(6)	2.150(2)
V−N(2)	2.140(3)	2.1336(17)	2.166(3)		
V−O(1)	1.897(2)	1.9038(14)	1.907(2)	1.890(5)	1.9289(17)
V−O(2)	1.910(2)	1.9079(14)	1.897(2)		
V−O(3)	2.146(2)	2.1366(13)	2.184(2)		2.148(3)
V−Cl	2.3405(10)	2.3317(6)	2.3303(10)	2.261(4)	2.2826(11)
			Bond Angles		
O(1)−V−O(2)	171.53(10)	168.12(6)	93.30(10)	99.9(3)	163.88(11)
O(1)−V−O(3)	87.59(10)	83.83(6)	81.66(9)		81.94(5)
O(1)−V−N(1)	88.49(10)	88.46(7)	85.73(9)	86.9(2)	89.00(8)
O(1)−V−N(2)	91.29(10)	90.47(6)	94.84(9)	95.8(2)	89.90(8)
O(1)−V−Cl	94.06(8)	96.65(5)	167.58(8)	130.05(15)	98.06(5)
O(2)−V−O(3)	84.27(9)	84.30(6)	174.88(10)		
O(2)−V−Cl	94.14(7)	95.20(5)	97.56(8)		
O(3)−V−Cl	177.92(7)	178.65(5)	87.55(6)		180.0
N(1)−V−O(2)	93.64(10)	91.46(6)	83.52(9)		
N(1)−V−O(3)	88.76(10)	86.63(6)	96.95(9)		86.06(6)
N(1)−V−Cl	90.01(8)	94.64(5)	89.50(7)	87.86(16)	93.94(6)
N(1)−V−N(2)	177.91(11)	176.08(6)	171.63(10)	175.7(3)	172.13(11)
N(2)−V−O(2)	86.88(10)	88.82(6)	88.11(10)		88.99(8)
N(2)−V−O(3)	93.30(10)	89.51(6)	91.39(9)		
N(2)−V−Cl	87.94(8)	89.23(5)	91.54(7)		

Dark red crystals of complexes **3b**, **3c**, **3e**, **3j**, and **3k** suitable for X-ray crystallographic analysis were grown from the chilled THF−hexane mixture solution, and their molecular structures were further confirmed by X-ray crystallographic analysis. The selected bond angles and distances of complexes **3b**, **3c**, **3e**, **3j**, and **3k** are summarized in Table 2. The molecular structures of **3b**, **3e**, and **3j** are shown in Figures 2–4, respectively, and those of **3c** and **3k** are shown in Figures S5 and S6 in the Supporting Information, respectively. Similar to complexes **2a**, **2b**, **2g**, **2i**, and **2k**, complexes **3b**, **3c**, **3e**, and**3k** also have a six-coordinate distorted octahedral geometry around the vanadium metal center.

As shown in Figures 2, S5, and S6, complexes **3b**, **3c**, and **3k** display similar molecular configurations. They all have a six-coordinate distorted octahedral geometry around the V metal center, in which the equatorial positions are occupied by oxygen and

(27) Gambarotta, S.; Mazzanti, M.; Floriani, C.; Chiesi-Villa, A.; Guastini, C. *Inorg. Chem.* **1986**, *25*, 2308.

(28) The THF is liberated while heating in vacuo at 120 °C in the amidinate vanadium(III) complexes (see ref 9).

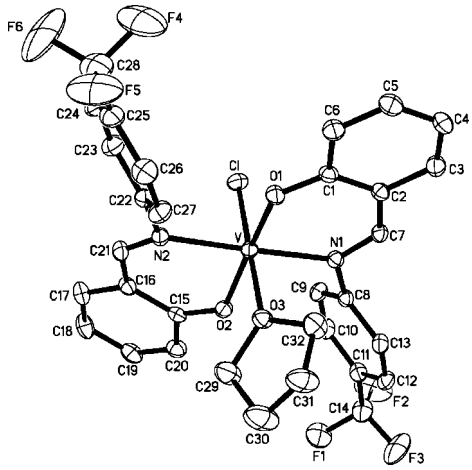

Figure 2. ORTEP drawing for complex **3b**. Thermal ellipsoids are drawn at the 30% probability level, and H atoms are omitted for clarity.

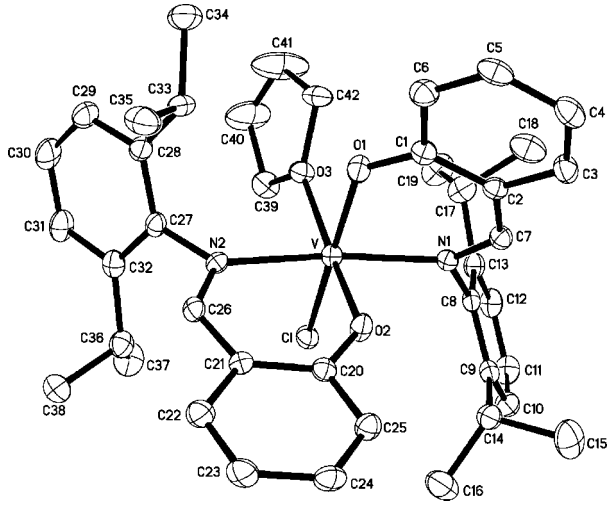

Figure 3. ORTEP drawing for complex **3e**. Thermal ellipsoids are drawn at the 30% probability level, and H atoms are omitted for clarity.

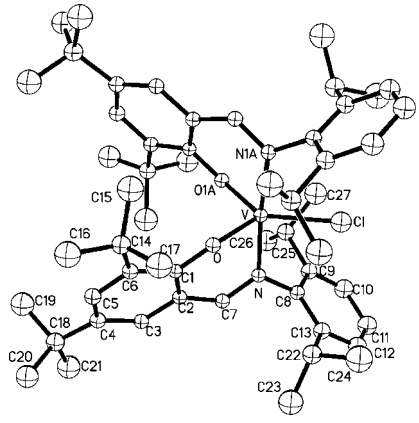

Figure 4. ORTEP drawing for complex **3j**. Thermal ellipsoids are drawn at the 30% probability level, and H atoms are omitted for clarity.

nitrogen atoms of two chelating salicyladiminato ligands. The chlorine atom is coordinated on the axial position, and the THF occupies another axial position, as seen in the bond angles for O(3)−V−Cl (around 179°), O(1)−V−O(2) (**3b**, 171.5°; **3c**, 168.1°; and **3k**, 163.9°), and N(1)−V−N(2) (**3b**, 177.9°; **3c**, 176.1°; and **3k**, 172.1°). The V−O and V−N bond distances in complex **3k** (1.929 and 2.150 Å) are slightly longer than those in complexes **3b** (1.897/1.910 and 2.122/2.140 Å), **3c** (1.904/1.908 and 2.129/2.134 Å), and V(salophen)Cl(THF) (1.894/1.909 and 2.084/2.109 Å) reported by Gambarotta.[27] A small but significant lengthening of the V−O and V−N bond distances in vanadium complexes **3b** and **3k** in contrast with those in their analogues **2b** (1.865 and 2.116 Å) and **2k** (1.881 and 2.107 Å) were observed because the two coordinated ligands repulsed each other.

Compared with complex **3b**, complex **3e** displays different geometry, in which the equatorial positions are occupied by two oxygen atoms of the salicyladiminato ligand and an additional oxygen atom of the THF molecule as well as chlorine atoms. Two nitrogen atoms are coordinated on the axial position. The DFT calculation indicates that in complex **3e** the THF and Cl prefer to exhibit a *cis* configuration (27.11 kJ/mol lower than the corresponding *trans* configuration), although the *trans* configuration of complex **3b** showed relatively lower formation energy (11.77 kJ/mol) than the *cis* configuration (see Table S1 in the Supporting Information). The V−N (2.187 and 2.166 Å) and V−O_3 (THF) (2.184 Å) bond distances in complex **3e** are longer than those in complexes **3b**, **3c**, and **3k**.

Interestingly, different from complexes **3b**, **3c**, **3e**, and **3k**, complex **3j** has a five-coordinate distorted trigonal-bipyramidal geometry; no THF molecule is coordinated around the vanadium metal center due to the steric effects of the ligands, which is also established by mass spectra and elemental analysis. The equatorial positions are occupied by two oxygen atoms and a chlorine atom. The nitrogen atoms are coordinated on the axial position. These results indicate that the steric effect of the ligand significantly influenced the structure of the bis(salicylaldiminato) vanadium complexes. Compared with complex **3e**, although additional obstacles were introduced in the aryloxy group in complex **3j**, the V−N bond distances (2.117 Å) in complex **3j** are somewhat shorter since there is no repulsion from the coordinated THF. The V−Cl bond distances in **3j** (2.261 Å) and **3k** (2.2826 Å) are shorter than those in **3b** (2.3405 Å), **3c** (2.3317 Å), and **3e** (2.3303 Å).

3. Ethylene Polymerization Screening Results. A great deal of research has shown that cocatalysts play an important role in vanadium catalysts. Halogen-containing alkylaluminium compounds such as Et_2AlCl, $Et_3Al_2Cl_3$, $EtAlCl_2$, and Me_2AlCl were effective cocatalysts for vanadium catalysts in ethylene homo- and copolymerization.[6b,7c,17a,d,e,21] Et_2AlCl was proved to be an efficient cocatalyst in the N,O chelate β-enaminoketonato vanadium catalytic systems; thus we chose it as the cocatalyst and optimized reaction conditions with complexes **2a** and **3a**. We found that the highest activities for ethylene polymerization appeared when the Al/V (mol/mol) equals 3000−4000 (Figure 5). However, the molecular weights of the polymer obtained gradually decreased with the increase of Et_2AlCl concentration. This indicates that chain transfer to aluminum took place during the polymerization.

Complexes **2a**−**k** and **3a**−**k** have been investigated as effective catalysts for ethylene polymerization under atmospheric pressure. As shown in Figures 6–9, ligand structure, complex model, and reaction temperature considerably influence catalytic activities and the molecular weights of the polymers obtained.

Although the structures of complexes **2a**−**e** are rather different, they display comparable catalytic activities (17−22 $\times$ 10^3 kg PE/mol$_V$·h·bar) toward ethylene polymerization at 25 °C. On introducing one *para*-trifluoromethyl (electron-withdrawing group) or *para*-methyl (donating group) into the N-aryl moiety of the ligand, to form complex **2b** or **2c**, catalytic

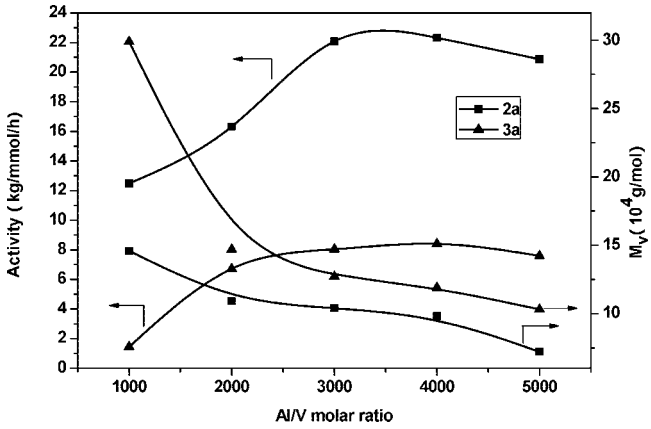

Figure 5. Plot of catalytic activity of vanadium complexes and viscosity-average molecular weight of the polymers obtained vs Al/V (molar ratio). Reaction conditions: 0.5 μmol of vanadium complex, Cl_3CCO_2Et 0.15 mmol, ethylene 1 bar, toluene 50 mL, at 25 °C, polymerization for 5 min.

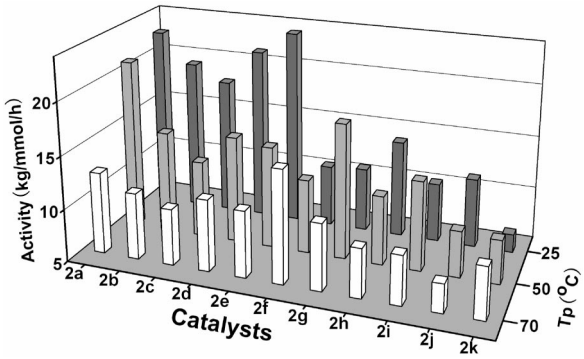

Figure 6. Catalytic activities of complexes **2a**−**k** toward ethylene polymerization at different temperatures. Reaction conditions: 0.5 μmol of vanadium complex, Cl_3CCO_2Et 0.15 mmol, Et_2AlCl 2 mmol, ethylene 1 bar, toluene 50 mL, polymerization for 5 min.

activity did not increase but decreased about 10%, and on introducing two *ortho*-isopropyls (bulky group) into the N-aryl moiety of the ligand, to form complex **2e**, catalytic activity increased about 10%. It is noteworthy that the catalytic activities of complexes **2b**−**e** rapidly decrease with an increase in temperature, but complex **2a** displays quite high activity at 50 °C, which is comparable with that at room temperature. Interestingly, with the introduction of a nonconjugated substituent cyclohexyl into the N-moiety of the ligand, complex **2f** exhibited much lower catalytic activity (10.8×10^3 kg PE/$mol_V \cdot h \cdot bar$) than **2a** (22.3×10^3 kg PE/$mol_V \cdot h \cdot bar$) at 25 °C, but different from complexes **2a**−**e**, complex **2f** displayed the highest catalytic activity toward ethylene polymerization at 70 °C. The molecular weights of the polymers obtained by complexes **2a**−**f** are comparable, and all decrease with an increase of reaction temperature.

Compared with complexes **2a** and **2e**, the complexes **2g**−**j**, bearing bulky *tert*-butyl on the aryloxy moiety of the ligand, showed much lower catalytic activities. This implies that the steric effect of the aryloxy moiety of the ligand would suppress a chain propagation reaction to some extent, which is different from that of the N-aryl moiety of the ligand. In addition, compared with complexes **2g** and **2i**, complexes **2h** and **2j** produced higher molecular weight polymers under the same conditions especially at high reaction temperature, indicating that the steric effect of the N-moiety of the ligand can suppress chain transfer reaction. On introducing two bromine atoms into

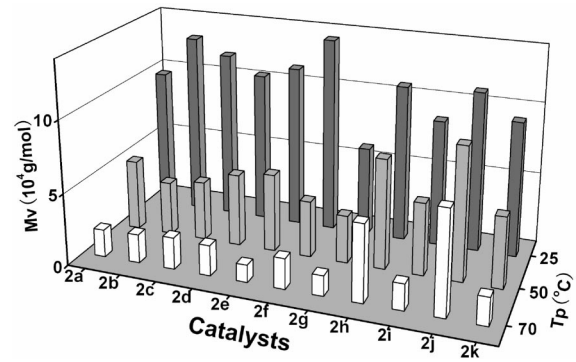

Figure 7. Viscosity-average molecular weight of the polyethylenes obtained by complexes **2a**−**k** at different temperatures. Reaction conditions: 0.5 μmol of vanadium complex, Cl_3CCO_2Et 0.15 mmol, Et_2AlCl 2 mmol, ethylene 1 bar, toluene 50 mL, polymerization for 5 min.

the aryloxy moiety of the ligand, complex **2k** displayed the lowest catalytic activity (9.12×10^3 kg PE/$mol_V \cdot h \cdot bar$) among 11 salicyladiminato vanadium complexes, and the molecular weight of the polymers obtained under the same conditions are comparable with those obtained by other complexes. It seems that both electronic and steric effects play a role toward the decrease of catalytic activity for ethylene polymerization with the salicyladiminato vanadium complexes.

All bis(salicyladiminato) vanadium complexes are effective catalyst precursors for ethylene polymerization, although they show lower catalytic activities than the corresponding salicyladiminato complexes at low reaction temperature (Figure 8). Different from the case of complexes **2a**−**k**, the structures of the ligand in **3a**−**k** greatly affect catalysis behavior of these bis(salicyladiminato) vanadium complexes toward ethylene polymerization.

Compared with complex **3a**, complexes **3b** and **3k**, bearing CF_3-substituted and diBr-substituted salicyladiminato ligands, respectively, exhibited higher catalytic activities, indicating that electron-withdrawing effects can improve catalytic performance of the bis(salicyladiminato) vanadium complexes, which is different from the case of the corresponding salicyladiminato vanadium complexes. It is noteworthy that the catalytic activities of complexes **3d** and **3e** are much higher than that of complex **3a** under the same conditions, which shows that the steric effects of the N-moiety of the salicyladiminato ligands can improve vanadium catalyst performance. Furthermore, the catalytic activities of complexes **3g** and **3i** are also higher than that of complex **3a**, which shows that the steric effects of the aryloxy moiety of the ligands also ameliorate vanadium catalyst performance. However, complexes **3h** and **3j** display only extremely low catalytic activities. The molecular structure of **3j** (Figure 4) may shed some light on this result. The bulky substituents on both the N-moiety and aryloxy moiety of the salicyladiminato ligand, which have excluded the THF molecule from the vanadium center, probably hinder the ethylene insertion reaction. Interestingly, complex **2f**, with nonconjugated cyclohexyl on the N-moiety of the ligand, exhibited higher catalytic activity than complex **2a** at 50 and 70 °C.

Although the molecular weights of the polymers obtained by the bis(salicyladiminato) vanadium complexes at high reaction temperature are also much lower than those obtained at low reaction temperature (Figure 9), the bis(salicyladiminato) vanadium complexes, except **3h** and **3j**, all display similar or even higher catalytic activities at high reaction temperature than at low temperature, which is completely different from the case of the corresponding salicyladiminato complexes **2a**−**k**. Moreover, with the increase of

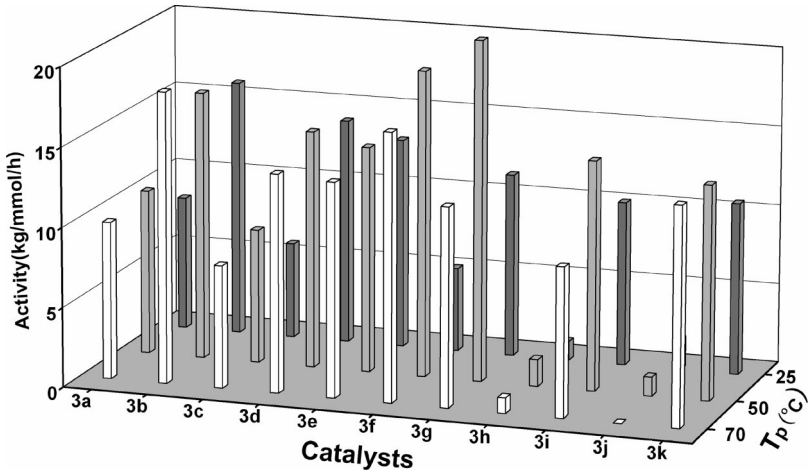

Figure 8. Catalytic activities of complexes **3a**−**k** toward ethylene polymerization at different temperatures. Reaction conditions: 0.5 μmol of vanadium complex, Cl_3CCO_2Et 0.15 mmol, Et_2AlCl 2 mmol, ethylene 1 bar, toluene 50 mL, polymerization for 5 min.

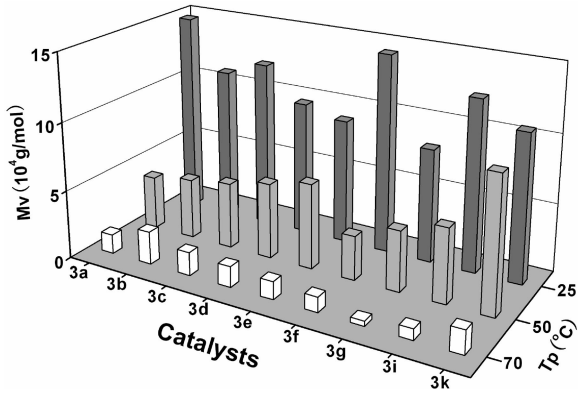

Figure 9. Viscosity-average molecular weights of the polyethylenes obtained by complexes **3a**−**k** at different temperatures. Reaction conditions: 0.5 μmol of vanadium complex, Cl_3CCO_2Et 0.15 mmol, Et_2AlCl 2 mmol, ethylene 1 bar, toluene 50 mL, polymerization for 5 min.

reaction temperature, the molecular weight distribution of the polymers produced by the salicyladiminato complexes such as **2a** dramatically broaden (from 2.7 to 12.0, entries 1−3 in Table 3), while those obtained by the bis(salicyladiminato) complexes such as **3a** only slightly broaden (from 1.9 to 2.6, rntries 9−11 in Table 3). In addition, the catalytic activities of the salicyladiminato complexes such as **2a** sharply decline with prolonged reaction time, while those of the bis(salicyladiminato) complexes such as **3a** only slightly decrease, as shown in Figure 10. These results indicate that two salicyladiminato ligands can stabilize active species and maintain single-site catalytic behaviors of the vanadium catalyst for ethylene polymerization.

Conclusions

Vanadium(III) complexes bearing one or two salicyladiminato ligands can be synthesized by controlling the molar ratio of $VCl_3(THF)_3$ and ligand. Molecular structures show that the substituents on the salicyladiminato have a slight effect on the configuration of the monosalicyladiminato vanadium complexes, while the steric obstacles influence the configuration of the bis(salicyladiminato) vanadium complexes, which has been also established by DFT calculations. In the presence of Et_2AlCl, salicyladiminato vanadium complexes were highly active catalysts for ethylene polymerization at 25 °C, and with increasing the polymerization temperature the catalytic behavior varied depending on the substituents on the salicyladiminato. Screening of bis(salicyladiminato) vanadium complexes found high activities were available at high polymerization temperature by introducing an electron-withdrawing group or alkyl substituents into the N-moiety of the ligand. Narrow molecular weight distribution polymers were produced by bis(salicyladiminato) vanadium complexes at high polymerization temperature, indicating good thermal stability of the catalysts. These results clearly indicate that the substituents on both the N-moiety and aryloxy moiety directly affect the polymerization behavior of the vanadium complexes, although the exact active species is still unknown to date.

Experimental Section

General Procedures and Materials. All manipulation of air- and/or moisture-sensitive compounds was carried out under a dry argon atmosphere by using standard Schlenk techniques or under a dry argon atmosphere in an MBraun glovebox unless otherwise noted. All solvents were purified from an MBraun SPS system. The ^1H NMR spectra of the vanadium complexes were obtained on a Bruker 300 MHz spectrometer at ambient temperature, with CD_2Cl_2 as the solvent. The IR spectra were recorded on a Bio-Rad FTS-135 spectrophotometer. Elemental analyses were recorded on an elemental Vario EL spectrometer. Mass spectra were obtained using electron impact (EI-MS) and LDI-1700 (Linear Scientific Inc.). The DSC measurements were performed on a Perkin-Elmer Pyris 1 differential scanning calorimeter at a rate of 10 °C/min. The weight-average molecular weight (M_w) and the polydispersity index (PDI) of polymer samples were determined at 150 °C by a PL-GPC 220 type high-temperature chromatograph equipped with three Plgel 10 μm mixed-B LS type columns. 1,2,4-Trichlorobenzene (TCB) was employed as the solvent at a flow rate of 1.0 mL/min. The calibration was made by polystyrene standard EasiCal PS-1 (PL Ltd.). The intrinsic viscosity of the polymer sample was measured in decalin at 135 °C using an Ubbleohed viscometer, and the average molecular weight was calculated using the following equation.[29]

$$[\eta] = 6.2 \times 10^{-4}\, M_v^{0.7} \quad (1)$$

Ethyl trichloroacetate (ETA) was purchased from Aldrich, dried over calcium hydride at room temperature, and then distilled. Diethylaluminium chloride (DEAC) was obtained from Albemarle Corporation. $VCl_3(THF)_3$, phenol compounds, and amine compounds were purchased from Aldrich. Literature procedures were used to synthesize salicylaldiminato ligands.[24a]

(29) Chiang, R. J. *Polym. Sci.* **1957**, *28*, 235.

Table 3. Typical Results of Ethylene Polymerization by Complexes [RN=CH(ArO)]$VCl_2(THF)_2$ and [RN=CH(ArO)]$_2VCl(THF)_x$ as well as $VCl_3(THF)_3$[a]

entry	complex	time (min)	temperature (°C)	polymer(g)	activity[b]	M_w[c](× 10^4)	M_w/M_n[c]
1	**2a**	5	25	0.93	22.3	13.8	2.7
2	**2a**	5	50	0.88	21.1	5.7	3.8
3	**2a**	5	70	0.53	12.7	3.8	12.0
4	**2b**	5	50	0.61	14.6	4.7	3.7
5	**2e**	5	50	0.61	14.6	7.3	3.5
6	**2f**	5	50	0.50	12.0	5.4	3.2
7	**2g**	5	50	0.74	17.8	5.4	3.4
8	**2k**	5	50	0.38	9.12	5.8	4.0
9	**3a**	5	25	0.35	8.40	17.1	1.9
10	**3a**	5	50	0.43	10.3	6.1	2.2
11	**3a**	5	70	0.41	9.84	1.5	2.6
12	**3b**	5	50	0.70	16.8	5.7	2.8
14	**3b**	5	70	0.76	18.2	3.2	3.0
15	**3e**	5	50	0.59	14.2	7.0	2.4
16	**3f**	5	50	0.80	19.2	3.9	2.8
17	$VCl_3(THF)_3$	5	25	0.85	20.4	24.6	2.6
18	$VCl_3(THF)_3$	5	50	0.78	18.7	15.5	5.3
19	$VCl_3(THF)_3$	5	70	0.40	9.60		

[a] Reaction conditions: 1 bar of ethylene pressure, 0.5 μmol of vanadium complex, Cl_3CCO_2Et/V (molar ratio) = 300, Al/V (molar ratio) = 4000, toluene 50 mL. [b] kg of PE/mmol$_V$·h·bar. [c] Weight-average molecular weight and polydispersity index of the resultant polyethylene determined by high-temperature GPC using polystyrene standard.

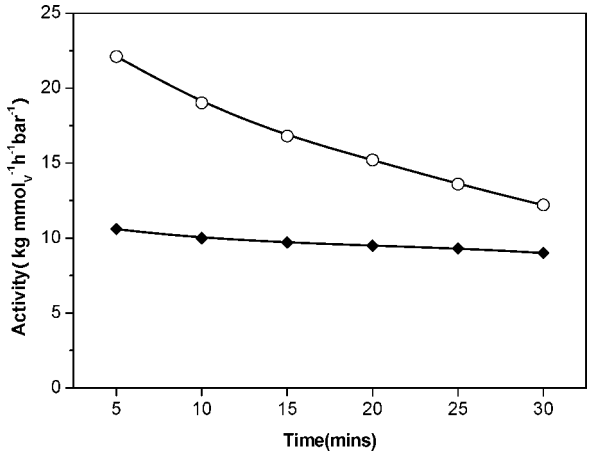

Figure 10. Lifetime plot of ethylene polymerization for complexes **2a** (○) and **3a** (◆) at 50 °C. Reaction conditions: 0.1 μmol of vanadium complex, Cl_3CCO_2Et 0.03 mmol, Et_2AlCl 0.4 mmol, ethylene 1 bar, toluene 50 mL.

Synthesis of Vanadium Complexes. [C_6H_5N=CH(C_6H_4O)]$VCl_2(THF)_2$ (2a). To a stirred solution of $VCl_3(THF)_3$ (0.75 g, 2.0 mmol) in dried tetrahydrofuran (20 mL) was added slowly a solution of 2-(PhNCH)C_6H_4OH (0.40 g, 2.0 mmol) in tetrahydrofuran (20 mL). The red reaction mixture was stirred for 10 min, and Et_3N (0.3 mL, 216 mg, 2.1 mmol) was added. After stirring for 4 h at room temperature the solution was concentrated to about 10 mL, and then the mixture was filtered to remove NH_4Cl. Crystallization by diffusion of *n*-hexane (20 mL) into the clear solution yielded red-black crystals of **2a** (0.65 g, 70%). Compound **2b**−**k** were prepared analogously. Mp: 148−150 °C. IR (KBr pellets): ν 3058, 2979, 2895, 1607, 1586, 1544, 1487, 1452, 1441, 1384, 1320, 1295, 1286, 1255, 1227, 1186, 1177, 1150, 1080, 1024, 975, 939, 918, 876, 850, 801, 764, 752, 702, 637, 590, 544, 531, 493, 463, 404 cm^{-1}. EI-MS (70 eV): *m*/*z* 459 [M^+]. Anal. Calcd for $C_{21}H_{24}Cl_2NO_3V$: C, 54.80; H, 5.26; N, 3.04. Found: C, 54.65; H, 5.16, N, 3.09.

[*p*-$CF_3C_6H_4N$=CH(C_6H_4)]$VCl_2(THF)_2$ (2b). Yield: 70%. Mp: 165−167 °C. IR (KBr pellets): ν 3060, 2966, 2897, 1602, 1588, 1545, 1510, 1470, 1440, 1417, 1389, 1378, 1325, 1299, 1251, 1227, 1179, 1151, 1109, 1068, 1015, 987, 930, 867, 841, 807, 763, 672, 637, 611, 585, 549, 527, 496, 472, 445 cm^{-1}. EI-MS (70 eV): *m*/*z* 527 [M^+]. Anal. Calcd for $C_{22}H_{23}F_3Cl_2NO_3V$: C, 50.02; H, 4.39; N, 2.65. Found: C, 50.29; H, 4.44, N, 2.58.

[*p*-MeC_6H_4N=CH(C_6H_4O)]$VCl_2(THF)_2$ (2c). Yield: 60%. Mp: 161−163 °C. IR (KBr pellets): ν 3056, 2983, 2956, 2885, 1610, 1599, 1589, 1543, 1507, 1469, 1436, 1387, 1342, 1333, 1294, 1255, 1231,1212, 1189, 1179, 1148, 1123, 1020, 979, 953, 928, 863, 834, 806, 758, 715, 680, 639, 625, 588, 532, 504, 495, 469, 425 cm^{-1}. EI-MS (70 eV): *m*/*z* 473 [M^+]. Anal. Calcd for $C_{22}H_{26}Cl_2NO_3V$: C, 55.71; H, 5.53; N, 2.95. Found: C, 55.79; H, 5.60, N, 2.91.

[2,6-$Me_2C_6H_3N$=CH(C_6H_4O)]$VCl_2(THF)_2$ (2d). Yield: 63%. Mp: 155−158 °C. IR (KBr pellets): ν 2975, 2903, 1604, 1585, 1468, 1458, 1436, 1385, 1338, 1298, 1252, 1212, 1173, 1150, 1126, 1095, 1030, 1011, 984, 928, 879, 856, 811, 766, 737, 709, 671, 637, 613, 568, 522, 513, 458, 425 cm^{-1}. EI-MS (70 eV): *m*/*z* 487 [M^+]. Anal. Calcd for $C_{23}H_{28}Cl_2NO_3V$: C, 56.57; H, 5.78; N, 2.87. Found: C, 55.20; H, 5.91, N, 2.79.

[2,6-$iPr_2C_6H_3N$=CH(C_6H_4O)]$VCl_2(THF)_2$ (2e). Yield: 76%. Mp: 157−160 °C. IR (KBr pellets): ν 3049, 3016, 2964, 2927, 2869, 1604, 1584, 1542, 1465, 1442, 1385, 1373, 1359, 1339, 1390, 1330, 1290, 1249, 1210, 1169, 1151, 1126, 1111, 1093, 1058, 1044, 1029, 1014, 991, 941, 929, 911, 894, 854, 796, 762, 757, 701, 674, 617, 550, 533, 525, 460 cm^{-1}. EI-MS (70 eV): *m*/*z* 543 [M^+]. Anal. Calcd for $C_{27}H_{36}Cl_2NO_3V$: C, 59.57; H, 6.66; N, 2.57. Found: C, 60.10; H, 6.72, N, 2.53.

[$C_6H_{11}N$=CH(C_6H_4O)]$VCl_2(THF)_2$ (2f). Yield: 69%. Mp: 147−148 °C. IR (KBr pellets): ν 3046, 2927, 2853, 1611, 1546, 1471, 1447, 1414, 1357, 1338, 1322, 1291, 1270, 1245, 1208, 1146, 1121, 1076, 1061, 1043, 1022, 995, 969, 916, 872, 844, 820, 772, 740, 688, 631, 584, 544, 504, 490, 455, 426 cm^{-1}. EI-MS (70 eV): *m*/*z* 465 [M^+]. Anal. Calcd for $C_{21}H_{30}Cl_2NO_3V$: C, 54.09; H, 6.48; N, 3.00. Found: C, 54.15; H, 6.53, N, 2.96.

[C_6H_5N=CH(OC_6H_3*t*Bu-2)]$VCl_2(THF)_2$ (2g). Yield: 71%. Mp: 177−179 °C. IR (KBr pellets): ν 3064, 2966, 2896, 1603, 1588, 1549, 1489, 1451, 1421, 1388, 1314, 1286, 1265, 1185, 1146, 1090, 1027, 1016, 975, 921, 874, 854, 766, 750, 705, 692, 653, 561, 470, 408 cm^{-1}. EI-MS (70 eV): *m*/*z* 515 [M^+]. Anal. Calcd for $C_{25}H_{32}Cl_2NO_3V$: C, 58.15; H, 6.25; N, 2.71. Found: C, 58.30; H, 6.27, N, 2.75.

[2,6-*i*$Pr_2C_6H_3N$=CH(OC_6H_3*t*Bu-2)]$VCl_2(THF)_2$ (2h). Yield: 53%. Mp: 140−141 °C. IR (KBr pellets): ν 3063, 2959, 2869, 1599, 1588, 1544, 1464, 1438, 1416, 1382, 1362, 1289, 1265, 1197, 1166, 1147, 1088, 1002, 932, 877, 855, 800, 754, 680, 567, 540, 515,

476 cm^{-1}. EI-MS (70 eV): *m/z* 599 [M^+]. Anal. Calcd for $C_{31}H_{44}Cl_2NO_3V$: C, 62.00; H, 7.38; N, 2.33. Found: C, 61.92; H, 7.33, N, 2.35.

[C_6H_5N=CH($OC_6H_2tBu_2$-2,4)]$VCl_2(THF)_2$ (2i). Yield: 76%. Mp: 201−202 °C. IR (KBr pellets): *ν* 3054, 2947, 2901, 1608, 1591, 1542, 1488, 1460, 1432, 1388, 1358, 1300, 1273, 1253, 1192, 1173, 1135, 1024, 970, 927, 871, 843, 773, 752, 705, 694, 645, 568, 545, 518, 488, 417 cm^{-1}. EI-MS (70 eV): *m/z* 541 [M^+]. Anal. Calcd for $C_{29}H_{40}Cl_2NO_3V$: C, 60.84; H, 7.04; N, 2.45. Found: C, 60.75; H, 6.49, N, 2.47.

[2,6-$iPr_2C_6H_3N$=CH($OC_6H_2tBu_2$-2,4)]$VCl_2(THF)_2$ (2j). Yield: 64%. Mp: 156−158 °C. IR (KBr pellets): *ν* 3063, 2960, 2869, 1606, 1583, 1538, 1463, 1430, 1383, 1362, 1272, 1251, 1201, 1167, 1097, 1014, 932, 864, 843, 800, 764, 636, 572, 545, 462 cm^{-1}. EI-MS (70 eV): *m/z* 655 [M^+]. Anal. Calcd for $C_{35}H_{52}Cl_2NO_3V$: C, 64.02; H, 7.98; N, 2.13. Found: C, 64.12; H, 7.89, N, 3.01.

[C_6H_5N=CH($OC_6H_2Br_2$-2,4)]$VCl_2(THF)_2$ (2k). Yield: 62%. Mp: 168−169 °C. IR (KBr pellets): *ν* 3062, 2977, 2897, 1601, 1585, 1516, 1486, 1432, 1401, 1377, 1298, 1224, 1193, 1166, 1077, 1024, 1011, 973, 920, 848, 770, 745, 723, 703, 630, 544, 519, 438 cm^{-1}. EI-MS (70 eV): *m/z* 614 [M^+]. Anal. Calcd for $C_{21}H_{22}Cl_2NO_3V$: C, 40.81; H, 3.59; N, 2.27. Found: C, 40.71; H, 3.64, N, 2.32.

[C_6H_5N=CH(C_6H_4O)]$_2$VCl(THF) (3a). To a stirred solution of $VCl_3(THF)_3$ (0.36 g, 1.0 mmol) in dried tetrahydrofuran (20 mL) was added slowly a solution of 2-(PhNCH)C_6H_4OH (0.40 g, 2.0 mmol) in tetrahydrofuran (20 mL). The red reaction mixture was stirred for 20 min, and Et_3N (0.3 mL, 216 mg, 2.1 mmol) was added. After stirring overnight at room temperature the solution was concentrated to about 10 mL and then the mixture was filtered to remove NH_4Cl. Crystallization by diffusion of *n*-hexane (20 mL) into the clear solution and chilling the solution (−40 °C) yielded 352 mg of **3a** (64%) as red-brown crystals. Compounds **3b**−**k** were prepared analogously. Mp: 170−172 °C. IR (KBr pellets): *ν* 3050, 2972, 2898, 1949, 1605, 1589, 1542, 1487, 1470, 1443, 1386, 1336, 1303, 1254, 1227, 1184, 1148, 1122, 1077, 1027, 977, 934, 906, 871, 854, 803, 760, 698, 657, 629, 585, 545, 521, 496, 464 cm^{-1}. EI-MS (70 eV): *m/z* 549 [M^+]. Anal. Calcd for $C_{30}H_{28}ClN_2O_3V$: C, 65.40; H, 5.12; N, 5.08. Found: C, 64.89; H, 4.97, N, 5.14.

[*p*-$CF_3C_6H_4N$=CH(C_6H_4O)]$_2$VCl(THF) (3b). Yield: 51%. Mp: 219−220 °C. IR (KBr pellets): *ν* 3047, 2979, 2902, 1602, 1589, 1544, 1510, 1469, 1442, 1416, 1396, 1378, 1326, 1297, 1257, 1229, 1189, 1177, 1162, 1153, 1147, 1122, 1107, 1067, 1028, 1016, 988, 927, 864, 847, 841, 822, 808, 761, 744, 672, 628, 610, 582, 568, 547, 500, 462, 446 cm^{-1}. EI-MS (70 eV): *m/z* 686 [M^+]. Anal. Calcd for $C_{32}H_{26}ClF_6N_2O_3V$: C, 55.95; H, 3.81; N, 4.08. Found: C, 56.25; H, 3.71, N, 4.01.

[*p*-MeC_6H_4N=CH(C_6H_4O)]$_2$VCl(THF) (3c). Yield: 69%. Mp: 203−205 °C. IR (KBr pellets): *ν* 3043, 3021, 2977, 2917, 1611, 1598, 1587, 1543, 1505, 1468, 1441, 1391, 1377, 1333, 1296, 1251, 1223, 1185, 1175, 1146, 1122, 1111, 1065, 1031, 1019, 980, 925, 881, 862, 830, 800, 756, 740, 713, 634, 618, 586, 525, 502, 457, 427, 414 cm^{-1}. EI-MS (70 eV): *m/z* 578 [M^+]. Anal. Calcd for $C_{32}H_{32}ClN_2O_3V$: C, 66.38; H, 5.57; N, 4.84. Found: C, 66.68; H, 5.48, N, 4.81.

[2,6-$Me_2C_6H_3N$=CH(C_6H_4O)]$_2$VCl(THF) (3d). Yield: 30%. Mp: 188−189 °C. IR (KBr pellets): *ν* 2948, 2903, 1611, 1604, 1585, 1542, 1466, 1442, 1390,1383, 1350, 1341, 1318, 1302, 1241, 1221, 1208, 1169, 1149, 1125, 1093, 1059, 1033, 1010, 985, 942, 927, 854, 843, 812, 777, 762, 751, 737, 708, 674, 632, 624, 605, 520, 510, 500, 457, 423 cm^{-1}. EI-MS (70 eV): *m/z* 606 [M^+]. Anal. Calcd for $C_{34}H_{36}ClN_2O_3V$: C, 67.27; H, 5.98; N, 4.61. Found: C, 67.55; H, 5.87, N, 4.60.

[2,6-$iPr_2C_6H_3N$=CH(C_6H_4O)]$_2$VCl(THF) (3e). Yield: 66%. Mp: 212−214 °C. IR (KBr pellets): *ν* 3060, 2954, 2923, 2863, 1607, 1544, 1470, 1438, 1391, 1382, 1361, 1348, 1339, 1332, 1311, 1297, 1251, 1210, 1168, 1152, 1148, 1124, 1107, 1094, 1058, 1043, 4032, 1022, 955, 926, 867, 854, 812, 793, 758, 702, 649, 629, 613, 532, 516, 457 cm^{-1}. EI-MS (70 eV): *m/z* 718 [M^+]. Anal. Calcd for $C_{42}H_{52}ClN_2O_3V$: C, 70.13; H, 7.29; N, 3.89. Found: C, 70.59; H, 7.22, N, 3.96.

[$C_6H_{11}N$=CH(C_6H_4O)]$_2$VCl(THF) (3f). Yield: 62%. Mp: 159−160 °C. IR (KBr pellets): *ν* 3050, 2921, 2850, 1618, 1598, 1554, 1518, 1473, 1447, 1414, 1357, 1319, 1287, 1264, 1252, 1216, 1207, 1150, 1123, 1074, 1050, 1033, 994, 967, 943, 914, 890, 857, 852, 843, 823, 791, 756, 737, 691, 650, 639, 582, 545, 497, 457, 427 cm^{-1}. EI-MS (70 eV): *m/z* 562 [M^+]. Anal. Calcd for $C_{30}H_{40}ClN_2O_3V$: C, 64.00; H, 716; N, 4.98. Found: C, 64.20; H, 7.02, N, 4.99.

[C_6H_5N=CH(OC_6H_3tBu-2)]$_2$VCl(THF) (3g). Yield: 42%. Mp: 191−193 °C. IR (KBr pellets): *ν* 3065, 2948, 2904, 2868, 1601, 1590, 1544, 1485, 1461, 1451, 1419, 1383, 1355, 1332, 1321, 1297, 1265, 1243, 1183, 1144, 1088, 1029, 979, 911, 874, 854, 809, 770, 763, 751, 701, 687, 646, 621, 614, 605, 548, 462, 404 cm^{-1}. EI-MS (70 eV): *m/z* 662 [M^+]. Anal. Calcd for $C_{38}H_{44}ClN_2O_3V$: C, 68.82; H, 6.69; N, 4.22. Found: C, 68.95; H, 6.57, N, 4.16.

[2,6-$iPr_2C_6H_3N$=CH(OC_6H_3tBu-2)]$_2$VCl (3h). Yield: 56%. Mp: 161−164 °C. IR (KBr pellets): *ν* 3062, 2960, 2868, 1602, 1589, 1546, 1465, 1440, 1410, 1382, 1362, 1317, 1261, 1225, 1197, 1168, 1147, 1094, 1058, 1031, 975, 934, 873, 849, 799, 763, 752, 677, 631, 566, 539, 515, 476 cm^{-1}. EI-MS (70 eV): *m/z* 758 [M^+]. Anal. Calcd for $C_{46}H_{60}ClN_2O_2V$: C, 72.76; H, 7.96; N, 3.69. Found: C, 72.85; H, 8.04, N, 3.66.

[C_6H_5N=CH($OC_6H_2tBu_2$-2,4)]$_2$VCl(THF) (3i). Yield: 65%. Mp: 217−219 °C. IR (KBr pellets): *ν* 3057, 2960, 2903, 2867, 1608, 1585, 1548, 1533, 1487, 1460, 1431, 1384, 1361, 1317, 1303, 1273, 1255, 1192, 1169, 1138, 1079, 1026, 998, 978, 920, 905, 866, 835, 810, 784, 764, 745, 707, 695, 637, 557, 542, 531, 495, 474 cm^{-1}. EI-MS (70 eV): *m/z* 774 [M^+]. Anal. Calcd for $C_{46}H_{60}ClN_2O_3V$: C, 71.25; H, 7.80; N, 3.61. Found: C, 71.18; H, 7.83, N, 3.63.

[2,6-$iPr_2C_6H_3N$=CH($OC_6H_2tBu_2$-2,4)]$_2$VCl (3j). Yield: 61%. Mp: 174−175 °C. IR (KBr pellets): *ν* 3060, 2962, 2869, 1609, 1586, 1540, 1465, 1427, 1381, 1362, 1327, 1270, 1248, 1201, 1167, 1137, 1098, 1057, 1042, 979, 933, 872, 833, 799, 762, 635, 567, 546, 472 cm^{-1}. EI-MS (70 eV): *m/z* 870 [M^+]. Anal. Calcd for $C_{54}H_{76}ClN_2O_2V$: C, 74.41; H, 8.79; N, 3.21. Found: C, 74.29; H, 8.81, N, 3.19.

[C_6H_5N=CH($OC_6H_2Br_2$-2,4)]$_2$VCl(THF) (3k). Yield: 80%. Mp: 180−182 °C. IR (KBr pellets): *ν* 3049, 2953, 2870, 1601, 1585, 1515, 1486, 1438, 1400, 1377, 1297, 1224, 1190, 1165, 1065, 1026, 863, 847, 765, 747, 717, 696, 626, 607, 546, 533, 519, 505, 438 cm^{-1}. EI-MS (70 eV): *m/z* 861 [M^+]. Anal. Calcd for $C_{30}H_{24}Br_4ClN_2O_3V$: C, 41.58; H, 2.79; N, 3.23. Found: C, 41.30; H, 2.75, N, 3.22.

Ethylene Polymerization. Polymerization was carried out under atmospheric pressure in toluene in a 150 mL glass reactor equipped with a mechanical stirrer. Toluene (50 mL) was introduced into the nitrogen-purged reactor and stirred vigorously (600 rpm). The toluene was kept at a prescribed polymerization temperature, and then ethylene gas feed was started. After 15 min, a solution of Et_2AlCl in toluene and a solution of ETA in toluene were added and stirred for 5 min. Then a toluene solution of the vanadium complexes was added into the reactor with vigorous stirring (900 rpm) to initiate polymerization. After a prescribed time, acidic alcohol (10 mL) was added to terminate the polymerization reaction, and the ethylene gas feed was stopped. The resulting mixture was added to acidic alcohol. The solid polyethylene was isolated by filtration, washed with alcohol, and dried at 60 °C for 24 h in a vacuum oven.

Crystallographic Studies. Crystals for X-ray analysis were obtained as described in the preparations. The crystallographic data, collection parameters, and refinement parameters are listed in Tables 4 and 5. The crystals were manipulated in a glovebox. The intensity

Table 4. Crystal Data and Structure Refinements of Complexes 2a, 2b, 2g, 2i, and 2k

	2a	2b	2g	2i	2k
formula	$C_{21}H_{26}Cl_2NO_3V$	$C_{22}H_{25}Cl_2F_3NO_3V$	$C_{25}H_{34}Cl_2NO_3V$	$C_{29}H_{42}Cl_2NO_3V$	$C_{21}H_{24}Br_2Cl_2NO_3V$
fw	462.27	530.27	518.37	574.48	620.07
cryst syst	triclinic	triclinic	monoclinic	monoclinic	triclinic
space group	$P\bar{1}$	$P\bar{1}$	$P2_1/c$	$P2(1)/c$	$P\bar{1}$
a (Å)	7.4606(6)	7.6147(9)	7.5894(8)	10.7986(13)	7.7892(7)
b (Å)	11.4975(9)	12.0671(14)	13.7589(14)	21.683(3)	11.9960(11)
c (Å)	13.9387(11)	13.7396(16)	24.542(3)	12.8415(15)	13.9022(13)
α (deg)	109.7700(10)	67.631(2)	90.00	90.00	106.9170(10)
β (deg)	90.0490(10)	85.279(2)	96.350(2)	91.601(2)	92.6990(10)
γ (deg)	107.6790(10)	86.104(2)	90.00	90.00	103.1800(10)
V (Å^3)	1064.85(15)	1162.6(2)	2547.0(5)	3005.6(6)	1201.06(19)
Z	2	2	4	4	2
D_{calcd} (Mg/m^3)	1.442	1.515	1.352	1.270	1.715
absorp coeff (mm^{-1})	0.738	0.705	0.625	0.537	3.985
F(000)	480	544	1088	1216	616
cryst size (mm)	0.31 × 0.20 × 0.08	0.15 × 0.10 × 0.10	0.22 × 0.12 × 0.03	0.25 × 0.09 × 0.04	0.46 × 0.26 × 0.16
θ range (deg)	1.56 to 26.02	1.61 to 25.99	1.67 to 26.04	2.46 to 19.22	2.71 to 26.04
no. of reflns collected	5863	6542	14 127	15 534	6744
no. of indep reflns	4078 (R_{int} = 0.0128)	4440 (R_{int} = 0.0190)	5022 (R_{int} = 0.1164)	5294 (R_{int} = 0.0989)	4623 (R_{int} = 0.0124)
no. of data/restraints/params	4078/0/253	4440/0/289	5022/0/132	5294/0/331	4623/0/271
GOF on F^2	1.040	1.059	0.921	0.988	1.058
R_1	0.0398	0.0689	0.1686	0.0649	0.0406
wR_2	0.0998	0.1262	0.1016	0.1057	0.0895

Table 5. Crystal Data and Structure Refinements of Complexes 3b, 3c, 3e, 3j, and 3k

	3b	3c	3e	3j	3k·2THF
formula	$C_{32}H_{26}ClF_6N_2O_3V$	$C_{32}H_{32}ClN_2O_3V$	$C_{42}H_{52}ClN_2O_3V$	$C_{54}H_{76}ClN_2O_2V$	$C_{38}H_{40}Br_4ClN_2O_5V$
fw	686.94	578.99	719.25	871.59	1010.75
cryst syst	monoclinic	monoclinic	monoclinic	monoclinic	monoclinic
space group	$C2/c$	$P2_1/n$	$P2_1/n$	$C2/c$	$C2/c$
a (Å)	26.2027(16)	12.3342(7)	11.6439(8)	17.673(3)	23.1831(18)
b (Å)	14.5250(9)	13.3442(7)	22.3741(16)	27.429(5)	10.0939(8)
c (Å)	27.0211(17)	17.9276(10)	14.8894(11)	11.8280(19)	16.7657(13)
α (deg)	90	90	90	90.00	90.00
β (deg)	117.5080(10)	103.0480(10)	93.753(2)	93.019(4)	101.7550(10)
γ (deg)	90	90	90	90.00	90.00
V (Å^3)	9121.4(10)	2874.5(3)	3870.7(5)	5725.8(17)	3841.0(5)
Z	12	4	4	4	4
D_{calcd} (Mg/m^3)	1.501	1.338	1.234	1.094	1.748
absorp coeff (mm^{-1})	0.488	0.473	0.365	0.261	4.534
F(000)	4200	1208	1528	2036	2008
cryst size (mm)	0.26 × 0.19 × 0.05	0.34 × 0.24 × 0.15	0.15 × 0.14 × 0.06	0.65 × 0.16 × 0.06	0.38 × 0.19 × 0.10
θ range (deg)	1.65 to 25.55	1.83 to 25.53	1.65 to 25.35	2.16 to 17.70	1.79 to 26.04
no. of reflns collected	24 215	15 120	20 510	15 902	10 555
no. of indep reflns	8529 (R_{int} = 0.0498)	5331 (R_{int} = 0.0201)	7073 (R_{int} = 0.0717)	5650 (R_{int} = 0.1547)	3809 (R_{int} = 0.0242)
no. of data/restraints/params	8529/0/610	5331/0/354	7073/0/450	5650/0/132	5650/0/232
GOF on F^2	1.009	1.101	0.990	0.995	1.033
R_1	0.0556	0.0426	0.0584	0.1185	0.0374
wR_2	0.1274	0.1330	0.1185	0.3157	0.0754

data were collected with the ω scan mode (186 K) on a Bruker Smart APEX diffractometer with CCD detector using Mo Kα radiation (λ = 0.71073Å). Lorentz, polarization factors were made for the intensity data, and absorption corrections were performed using the SADABS program. The crystal structures were solved using the SHELXTL program and refined using full matrix least-squares. The positions of hydrogen atoms were calculated theoretically and included in the final cycles of refinement in a riding model along with attached carbons.

DFT Calculations. All the DFT results were obtained from calculations based on the Becke−Perdew exchange−correlation functional, using the Amsterdam Density Functional (ADF) program.[30,31] The standard double-ζ STO basis sets with one set of polarization functions were applied for H, C, N, O, and Cl atoms, while the standard triple-ζ basis sets were employed for the V atom. The calculations of singlet vanadium species were performed in a spin-restricted fashion.[32] All reported results were calculated in the gas phase.

Acknowledgment. The authors are grateful for a subsidy provided by the National Natural Science Foundation of China (Nos. 20734002 and 50525312) and by the Special Funds for Major State Basis Research Projects (No. 2005CB623800) from the Ministry of Science and Technology of China.

Supporting Information Available: ORTEP drawings for complexes **2a**, **2g**, **2i**, **2k**, **3c**, and **3k**. X-ray diffraction data for **2a**, **2b**, **2g**, **2i**, **2k**, **3b**, **3c**, **3e**, **3j**, and **3k** (as CIF). Cartesian coordinates and energies of all stationary points discussed in the text. This material is available free of charge via the Internet at http://pubs.acs.org.

OM800097B

(30) (a) Baerends, E. J.; Ellis, D. E.; Ros, P. *Chem. Phys.* **1973**, *2*, 41. (b) Baerends, E. J.; Ros, P. *Chem. Phys.* **1973**, *2*, 52.

(31) te Velde, G.; Baerends, E. J. J. *Comput. Chem.* **1992**, *99*, 84.

(32) Deng, L. Q.; Schmid, R.; Ziegler, T. *Organometallics* **2000**, *19*, 3069, and references therein.